Reassessment of Acarbose as a Transition State Analogue Inhibitor of Cyclodextrin Glycosyltransferase†

Renee Mosi,‡ Howard Sham,‡ Joost C. M. Uitdehaag,§ Richard Ruiterkamp,§ Bauke W. Dijkstra,§ and Stephen G. Withers*,‡

Department of Chemistry, University of British Columbia, 2036 Main Mall, Vancouver, British Columbia V6T 1Z1, Canada, and BIOSON Research Institute and Laboratory of Biophysical Chemistry, Groningen Biomolecular Sciences and Biotechnology Institute, University of Groningen, Nijenborgh 4, 9747 AG Groningen, The Netherlands

Received May 13, 1998; Revised Manuscript Received August 18, 1998

ABSTRACT: The binding of several different active site mutants of *Bacillus circulans* cyclodextrin glycosyltransferase to the inhibitor acarbose has been investigated through measurement of K_i values. The mutations represent several key amino acid positions, most of which are believed to play important roles in governing the product specificity of cyclodextrin glycosyltransferase. Michaelis−Menten parameters for the substrates α-maltotriosyl fluoride (αG3F) and α-glucosyl fluoride (αGF) with each mutant have been determined by following the enzyme-catalyzed release of fluoride with an ion-selective fluoride electrode. In both cases, reasonable correlations are observed in logarithmic plots relating the K_i value for acarbose with each mutant and both k_{cat}/K_m and K_m for the hydrolysis of either substrate by the corresponding mutants. This indicates that acarbose, as an inhibitor, is mimicking aspects of both the ground state and the transition state. A better correlation is observed for αGF ($r = 0.98$) than αG3F ($r = 0.90$), which can be explained in terms of the modes of binding of these substrates and acarbose. Re-refinement of the previously determined crystal structure of wild-type CGTase complexed with acarbose [Strokopytov, B., Penninga, D., Rozeboom, H. J., Kalk, K. H., Dijhuizen, L., and Dijkstra, B. W. (1995) *Biochemistry 34,* 2234−2240] reveals a binding mode consistent with the transition state analogue character of this inhibitor.

Transition state analogues have long provided a valuable tool for probing enzymatic mechanisms as well as providing a basis for the design of tight binding enzyme inhibitors. Their design is based on the principle that extra binding interactions develop between the enzyme and substrate in the transition state complex conferring reaction specificity and rate acceleration. Thus, analogues which mimic the substrate transition state structure should bind tightly. This transition state analogy, which was first proposed by Pauling in 1946 (*2*) and then further evolved by Lienhard (*3*) and Wolfenden (*4*), has provided the framework for the design of a wide variety of tight binding, reversible enzyme inhibitors. Key characteristics of sugar-based transition state analogue inhibitors for glycosidases are a positive charge, a trigonal anomeric center, and a half-chair-like conformation (*5*−*8*).

A useful way of determining whether a particular inhibitor is truly a transition state analogue or is just a fortuitously tight binding inhibitor involves probing the effects on the K_i value of modifications to the interactions between the enzyme and inhibitor and then probing the effects of equivalent modifications to the enzyme/substrate complex at the transition state, as revealed in k_{cat}/K_m values. If the effects on the inhibitor K_i value correlate well with the effects on substrate k_{cat}/K_m, then it can be concluded that the inhibitor is indeed a transition state analogue. This approach has been reviewed recently (*9*). Such modifications can be effected in two ways. One way involves the synthesis and kinetic evaluation of a series of modified substrates with the wild-type enzyme, along with measurement of K_i values for the identically modified inhibitors. The other approach involves the construction of a series of mutant enzymes, preferably mutated at sites thought to play a role in substrate recognition and catalysis, and then measurement of k_{cat}/K_m and K_i values with each mutant for a single substrate and transition state analogue inhibitor, respectively. The choice of approach depends primarily upon whether it is easier to generate mutant enzymes or modified substrates and inhibitors. The former approach has been used to demonstrate that a series of phosphonamidate peptide derivatives are indeed true transition state analogue inhibitors for zinc peptidases and thermolysin (*10*−*12*). Similarly, nojiritetrazoles were shown by this method to be true transition state analogues for a range of glycosidases (*7*). Using the same approach, 1-deoxynojirimycin and castanospermine were shown not to be transition state analogues for *Agrobacterium* sp. β-glucosidase but rather, tight binding fortuitous inhibitors (*13*). The latter approach has been applied to rat carboxypeptidase A (*12, 14*) and glucoamylase (*15*). It seemed possible that such an approach could be applied to interactions of the

† Funding was kindly provided by the Natural Sciences and Engineering Council of Canada.

* To whom correspondence should be addressed (Fax: 604-822-2847; email: withers@chem.ubc.ca).

‡ University of British Columbia.

§ University of Groningen.

10.1021/bi981109a CCC: $15.00
Published on Web 11/13/1998

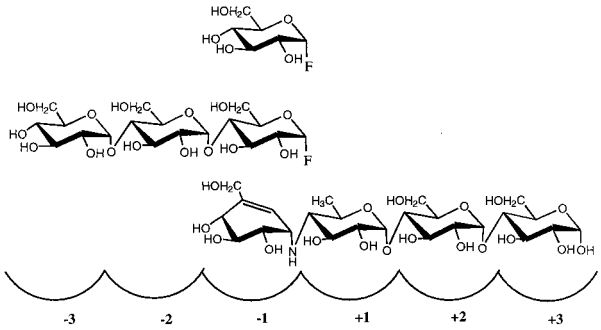

FIGURE 1: Structure of the pseudotetrasaccharide acarbose positioned in the subsites of CGTase in the 'amylase' mode with the relative binding positions of αG3F and αGF shown above. The cleavage site is positioned between subsites −1 and +1.

enzyme cyclodextrin glycosyltransferase (CGTase)[1] with the inhibitor acarbose to further understand the binding mode of acarbose to CGTase observed crystallographically (*16*).

CGTases are glycosyl transferases that degrade starch into linear or cyclic oligosaccharides (cyclodextrins). Much attention has been paid to these enzymes for their value in producing cyclodextrins, which have wide industrial applications (*17*). However, most CGTases suffer from a low product specificity, resulting in mixtures of most commonly α-, β- and γ-cyclodextrins which then require costly crystallization procedures for purification (*18*). Therefore, a great deal of effort has been expended to design CGTases with unique product specificities by generation of a number of mutants modified in the active site (*19, 20*). These enzymes belong to the same sequence- and structure-related family [Family 13; a $(\beta/\alpha)_8$ barrel] as do α-amylases and many α-glucosidases. As such, they are inhibited by the natural product acarbose, a pseudotetrasaccharide isolated from *Actinoplanes*, which has long been known as a potent reversible inhibitor of many Family 13 enzymes including the pig pancreatic α-amylase ($K_i = 10\ \mu$M) (*21*), as well as of the Family 15 glucoamylase ($K_i = 0.1$ nM) (*22*) (Figure 1). Indeed, it is currently used as a drug for the control of blood glucose levels in diabetics (*23*−*25*). Recently, the 2.5 Å crystal structure of a CGTase with acarbose bound at the active site was reported (*16*) as well as a structure of CGTase with a bound maltononaose inhibitor apparently derived from condensation of maltopentaose and acarbose (*26*). Interestingly, the mode of binding of acarbose appeared to be different from that in previously reported structures of complexes of acarbose with other α-glycosyl transferases/hydrolases, namely, glucoamylase, porcine pancreatic α-amylase, *Aspergillus oryzae* α-amylase (*27*−*29*), and a thermostable CGTase (*30*) since the valienamine moiety, generally thought to mimic the glycosyl cation-like transition state, does not appear to be bound in the −1 site in the case of CGTase.[2] Rather, it was interpreted to be bound in the −2 site, with the 6-deoxyglycosyl moiety bound in the −1 site and its glycosidic oxygen at the site of cleavage.

In an effort to investigate the interactions of acarbose with CGTase, we have screened a range of active site mutants which are believed to be responsible for governing a wide range of product specificities (Figure 2). Two substrates, α-maltotriosyl fluoride (αG3F) and α-glucosyl fluoride (αGF), were used in this analysis, allowing the determination of accurate kinetic parameters in a direct assay monitoring fluoride ion release (*31*). By correlating the kinetic parameters so determined with K_i values for acarbose, insights have been obtained into the nature of the strong inhibition afforded by this naturally occurring and therapeutically important inhibitor. In addition, to investigate whether an alternative binding mode of acarbose would be compatible with the original data set, the structure was re-refined.

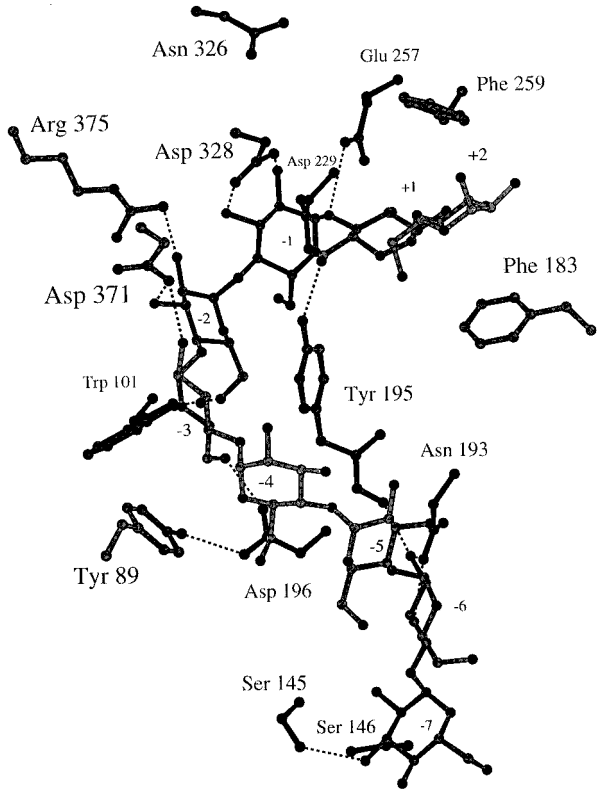

FIGURE 2: Active site of CGTase modeled with maltononaose bound showing the relative positions of the amino acid residues. [Diagram modeled on the crystal structure of a Y195F mutant complexed with an acarbose-derived maltononaose inhibitor (26)].

MATERIALS AND METHODS

General. All mutant CGTases were generated and purified as previously reported (*32*). αG3F and αGF were synthesized by the method of Junnemann et al. (*33*). All other chemicals were purchased from Sigma Chemical Co. with the exception of acarbose which was generously provided by Miles Inc. (now Bayer).

Kinetic Analysis. (A) Glycosyl Fluorides. The enzyme-catalyzed reactions were followed by monitoring the release of fluoride using an Orion fluoride-selective electrode interfaced to a pH/ion selective meter (Fischer Scientific). Data were collected using the program Terminal and analyzed using the program Grafit (*34*). In a typical experiment, αG3F or αGF was preincubated in 100 mM citrate buffer, pH 6.0, at 30 °C, for 10 min. The reaction was initiated by adding an appropriately diluted aliquot of enzyme in citrate buffer [final enzyme concentration with αG3F as substrate: wild-type (0.25 μg/mL); S145E (1.1 μg/

[1] Abbreviations: CGTase, cyclodextrin glycosyltransferase; αG3F, α-maltotriosyl fluoride; αGF, α-glucosyl fluoride; G, glucose; G2, maltose; G3, maltotriose; G4, maltotetraose; G5, maltopentaose; G6, maltohexaose; wt, wild-type.

[2] We are using the universal subsite nomenclature system recently proposed (*1*) in which cleavage occurs between the −1 and +1 subsites.

mL); S146P (13.4 μg/mL); D371N (1.7 μg/mL); N193G (1.5 μg/mL); N326Q (3.2 μg/mL); Y195G (3.2 μg/mL); Y195F (1.1 μg/mL); Y195L (1.1 μg/mL); with αGF as substrate: wild-type (0.25 μg/mL); S145E (19.3 μg/mL); S146P (416 μg/mL); D371N (97.3 μg/mL); N193G (65 μg/mL); N326Q (254 μg/mL); Y195G (276 μg/mL); Y195F (16.6 μg/mL); Y195L (28.1 μg/mL)] and the progress of the reaction monitored for approximately 5−10 min or until a maximum of 10% of substrate was consumed. For each enzyme, a total of seven substrate concentrations were analyzed, ranging from 0.2 to 5 times K_m. In almost all cases the kinetic constants K_m, V_{max}, and k_{cat} were calculated from a fit to the Michaelis−Menten equation using the program GraFit (*34*). For those mutants with very high K_m values (Y195G and N326Q), thus for which saturation behavior could not be observed, an accurate value of k_{cat}/K_m was obtained from the slope of the Lineweaver−Burk plot, and very approximate estimates of the individual parameters were obtained from the intercepts.

(B) Evaluation of Oligosaccharides as Acceptors. Differences in rate upon the addition of various maltooligosaccharide acceptors were determined by measuring the initial rate of D371N CGTase (10 μL aliquot, final concentration was 97.3 μg/mL) catalyzed fluoride release using a single concentration of αGF (40 μL aliquot, final concentration was 28 mM) in 100 mM citrate buffer, pH 6.0 (final volume before the addition of oligosaccharide was 260 μL). After following the reaction for 2 min, a 20 μL aliquot of the appropriate acceptor was added and the progress of the reaction monitored. Final concentrations of G to G6 were 30 mM.

(C) Inhibition of CGTases by Acarbose. Approximate K_i values for acarbose with each mutant were first determined by measuring the rate of enzyme-catalyzed fluoride release for a single concentration of αG3F or αGF at each of a series of concentrations of acarbose (6−8 concentrations), bracketing the K_i value so determined. The enzyme concentrations were identical to those used above for the respective substrate. The observed rates were plotted in the form of a Dixon plot ($1/v$ vs [acarbose]), and the K_i value was determined (assuming competitive inhibition) from the intercept of this line with the horizontal line drawn through $1/V_{max}$. In our experience, this approach consistently provides a K_i value close (within 20%) to that ultimately measured by a full analysis. Full K_i determinations were performed by measurements of V_{max} and K_m values at a series of inhibitor concentrations (typically five concentrations) which bracket the K_i value to be determined. The value of K_i and the mode of inhibition were determined through a direct fit of the data to expressions for each inhibition mode using the program GraFit (*34*).

Crystallographic Refinement. The CGTase−acarbose structure (cgtaca, PDB id code: 1cxg) was re-refined against the old data. To guard against overfitting, the free *R*-factor technique (*35*) was used, which was not available at the time the initial structure was refined. The structure of the CGTase mutant N193G (J. Uitdehaag, unpublished), without any ligands or waters, was taken as the starting model, because its cell parameters best resembled those of the cgtaca data set (*16*), with the same indices as the free *R*-factor set used for the N193G refinement, comprising 2248 reflections out of the total of 23 325.

Table 1: Quality of the Old and Re-refined CGTase + Acarbose Models

	old (1cxg) (*16*)	re-refined (cross-validated) (2cxg)
refinement statistics		
no. of nonsolvent atoms	5379	5401
no. of solvent atoms	192	92
average *B* factor (Å^2)	20.5	14.7
final *R* factor (%)[a]	15.1	18.2
final free *R* factor (%)[b]	−	23.7
Ramachandran outliers	0	0
coord error Luzzati (Å) (*47*)[c]	0.20	0.26
coord error σ_A (Å) (*44*)[c]	0.22	0.25
Procheck *G* factor (*38*)[d]	−0.47	0.17
root mean square deviation from ideal geometry		
bond lengths (Å)	0.011	0.004
bond angles (deg)	2.3	1.147
torsion angles (deg)	15.9	18.245
trigonal planes (Å)	0.015	0.004
planar groups (Å)	0.012	0.007
van der Waals contacts (Å)	0.028	0.009
neighboring atom *B* factor correlations (Å^2)	2.88	1.29

[a] R factor $= \Sigma_h|F_o - F_c|/\Sigma_h F_o$ where F_o and F_c are the observed and calculated structure factor amplitudes of reflection h, respectively. Reflections between 8.0 and 2.5 were used, with bulk solvent correction as implemented in TNT (*36*). The low R-factor of the old structure might indicate over refinement (*35*). [b] The free *R* factor is calculated as the *R* factor, using F_o that were excluded from the refinement. [c] Including all atoms. The error models are *R* factor based, which could explain the higher errors in the cross-validated structure. [d] A high value of the *G* factor indicates good overall stereochemistry.

For the actual refinement, the program TNT (*36*) was used in combination with O (*37*). The overall procedure for CGTase has been outlined previously (*30*). The number of refinable parameters was reduced by including only a few solvent oxygens, and keeping very tight restraints on the stereochemistry, which limits the degrees of freedom of bound atoms. At the beginning, the new initial structure had an *R*-factor of 34.0% and a free *R*-factor of 34.4%. In the course of refinement, and after model rebuilding (see below), this decreased to a final *R*-factor of 18.2% and a final free *R*-factor of 23.7%. This new *R*-factor is higher than in the old structure, but more in line with what is expected from 2.5 Å data (*35*). The new structure was analyzed with PROCHECK (*38*) and WHATCHECK (*39*), and had improved stereochemistry compared to the old model (see Table 1).

RESULTS AND DISCUSSION

Kinetic Analysis of Active Site Mutants of CGTase Using Glycosyl Fluorides as Substrates. As reported previously, both αG3F and αGF are convenient substrates for CGTase since the enzyme-catalyzed release of fluoride can be easily assayed using an ion-selective fluoride electrode (*31*). Even though CGTase otherwise prefers longer oligosaccharides, a short one, such as αGF, can be used if a good leaving group, such as fluoride, is provided. When the release of fluoride from αGF is followed using the fluoride electrode, a low reaction rate is observed over a lengthy induction period, but this rate gradually increases with time in an apparently sigmoidal manner, as is shown in Figure 3. It seemed likely that this behavior was a consequence of a transglycosylation reaction between two molecules of αGF

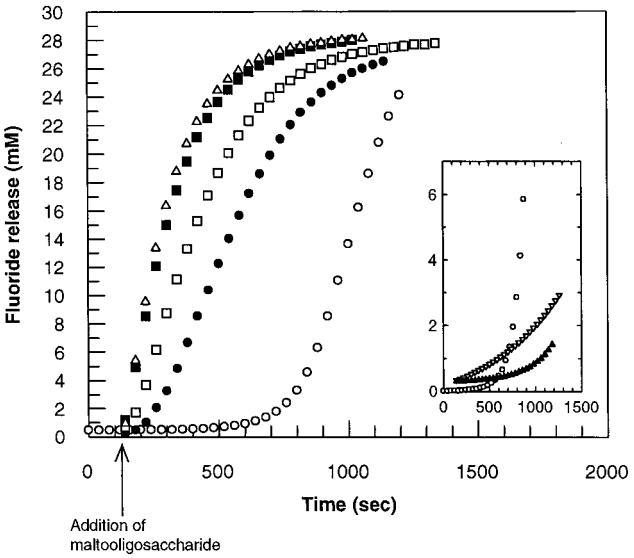

FIGURE 3: Reaction of D371N CGTase with αGF (28 mM) and various acceptors showing fluoride release over time. Concentrations of acceptors used were: ○ = no added acceptor; ● = 30 mM G3; □ = 30 mM G4; ■ = 30 mM G5; △ = 30 mM G6. Inset graph (expansion of main figure): ○ = no added acceptor; ▲ = 30 mM G; ▽ = 30 mM G2. The data for G and G2 have been displaced 0.36 mM above the actual initial concentration of fluoride to allow for easier visualization of the results.

producing maltosyl fluoride which acts as a better donor or acceptor, thereby more rapidly reacting to give αG3F and so on. The lack of such an induction period when αG3F was used as substrate (data not shown) certainly supports this hypothesis. Further evidence that longer oligosaccharides serve as better acceptors was obtained by monitoring the reaction with αGF in the presence of different maltooligosaccharides. As seen in Figure 3, inclusion of maltotriose considerably shortens the lag period while maltotetraose shortens it yet further. When maltopentaose or maltohexaose was added, no lag phase at all was observed. Since, in this study, we were interested in the rates of reaction of αGF, only the initial slope was used in our kinetic evaluation.

As shown in Table 2, a wide variety of mutations within the active site has been generated in an effort to determine the effect that a particular alteration has on the enzyme-catalyzed reaction. All of the mutants tested were able to utilize αG3F as a substrate, albeit to varying extents, with k_{cat} values ranging from 275 to 0.0093 s^{-1}, a spread of almost (3×10^4)-fold. Interestingly, K_m values for all the mutants studied were greater than that for the wild-type enzyme, indicating varying degrees of disruption of binding interactions. Consequently, k_{cat}/K_m values varied over an even larger range with a spread of (4.8×10^5)-fold. The degree of weakening of binding ranged from very small (<2-fold) in the cases of theY195F and S145E mutants to very large (80-fold) in the case of the Y195G mutant. This very small effect with the S145E mutant is consistent with the observation that this residue interacts only with the sugar residue in the −7 site (*26*). αG3F will not bind in that site; thus, effects should be minimal. The presence of very disparate effects with the Y195F and Y195G mutants is also consistent with the role of Y195. Y195 is thought to be the key amino acid in the active site which the cyclodextrin product wraps around during formation. It may also be largely responsible for helping to exclude water molecules from the active site, thus preventing hydrolysis (*26*). Its hydroxyl group is thought to hydrogen bond to the sugar in the +1 site, while the aromatic ring provides important interactions with the rest of the substrate, especially the sugar in the −1 site (*26*). Since αG3F does not occupy the +1 site, minor consequences of removing that hydrogen bond are reasonable, yet complete removal of the side chain is clearly highly deleterious.

Mutations within the CGTase system produced an even larger range of effects on the enzyme-catalyzed reaction of the shorter, monosaccharide substrate αGF; the k_{cat} values spanned from 330 to 0.0002 s^{-1}, a range of (1.6×10^6)-fold (Table 2). Effects on K_m ranged from a small disruption in binding (<1.5-fold) for the Y195F mutant to significant changes in binding (25-fold) for the Y195G mutant. Effects on k_{cat}/K_m consequently ranged over (4.1×10^7)-fold. Similar structure/activity correlations to those observed with αG3F are apparent. That is, the proximity of Y195 and N326 to the −1 subsite make them important residues for optimal binding of the substrate. N326 is known to sit in a key position in the active site, and kinetic analysis on mutants modified at the equivalent residue in a thermostable CGTase showed drastic changes in pH optima upon mutation (*30*). Therefore, mutations at these positions result in the largest disruptions in binding affinity and rate reductions.

Since this enzyme is a transferase, therefore ultimately requiring interactions in both the glycone and aglycone sites, care must be exercised in the interpretation of the kinetic parameters of these various mutants in terms of localized binding interactions. This is particularly true when the rate-determining step for each substrate/mutant combination is not known. If formation of the glycosyl enzyme is rate-limiting, then interactions in the negative (−1, −2, etc.) sites will likely be the most important. If, however, the second, transglycosylation step is rate-limiting, then interaction with the positive (+1, +2, etc.) sites could be equally important. This uncertainty is largely sidestepped if values of k_{cat}/K_m are interpreted since this second-order rate constant, known as the specificity constant, reflects only the first irreversible step. For CGTase utilizing glycosyl fluoride substrates, as shown with various glycosidases (*40*−*42*), it is reasonable to assume that this is the first, glycosylation step; thus, changes in k_{cat}/K_m reflect changes in interactions in the negative sites.

Inhibition of CGTase Mutants by Acarbose. Inhibition constants for acarbose were measured with each of the CGTase mutants, and these are also presented in Table 2. In three cases, including the weakest and strongest binding examples, the K_i value was determined from a full analysis using a range of substrate and inhibitor concentrations as is shown for Y195G CGTase in Figure 4. Inhibition was strictly competitive in each case. In the other cases, K_i values were determined from data obtained at a series of inhibitor concentrations using a fixed concentration of substrate as described under Materials and Methods. The mutant enzymes all bound to acarbose, but less tightly than does wild-type CGTase, with widely varying affinities ranging from a K_i of 0.2 μM for wild type to 341 μM for Y195G CGTase. This large loss of affinity upon removal of the Y195 side chain is again consistent with the key role played by this residue.

Table 2: Kinetic Parameters for the Reaction of α-Glucosyl Fluoride and α-Maltotriosyl Fluoride with CGTases (wt and Mutants) and for Inhibition by Acarbose

	α-glucosyl fluoride			α-maltotriosyl fluoride			
CGTase	K_m (mM)	k_{cat} (s^{-1})	k_{cat}/K_m (s^{-1} mM^{-1})	K_m (mM)	k_{cat} (s^{-1})	k_{cat}/K_m (s^{-1} mM^{-1})	acarbose K_i (mM)
wt	32.3[a]	330[a]	10.2[a]	2.5[a]	275[a]	110[a]	0.0002
Y195F	40.0	123	3.075	4.0	7.8	1.95	0.00036
Y195L	100	0.60	0.006	11.6	0.47	0.041	0.0176
Y195G	800	2×10^{-4}	2.5×10^{-7}	200	0.046	0.00023	0.341
N326Q	400	4.8×10^{-3}	1.2×10^{-5}	12.2	0.0093	0.00076	0.106
S145E	60	100	1.67	3.37	175	51.9	0.001
S146P	250	0.16	6.4×10^{-4}	16.5	7.75	0.470	0.025
D371N	74	1.35	0.0182	18.6	214	11.5	0.010
N193G	50	0.54	0.0108	7.65	57.6	7.52	0.005

[a] Reported previously (*31*).

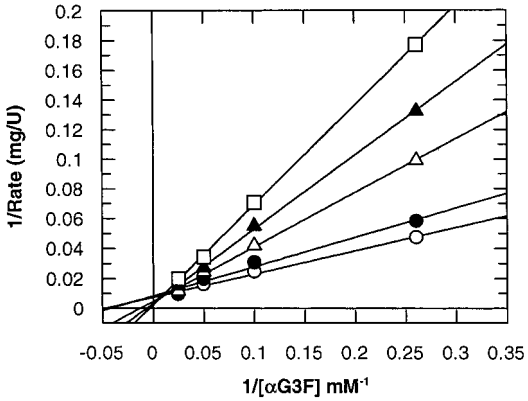

FIGURE 4: Lineweaver−Burk plot for Y195G CGTase with αG3F as substrate and acarbose as inhibitor. Concentrations of acarbose used were: ○ = 0 μM; ● = 38 μM; △ = 200 μM; ▲ = 384 μM; □ = 770 μM.

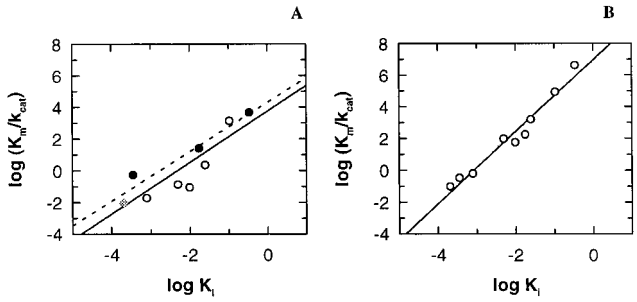

FIGURE 5: Linear free energy relationship between kinetic parameters for the inhibitor acarbose and glycosyl fluoride substrates with a series of mutants of CGTase. (A) log (K_m/k_{cat}) for αG3F vs log K_i for acarbose; (B) log (K_m/k_{cat}) for αGF vs log K_i for acarbose. (Filled circles represent Tyr mutants. The grey shaded circle represents wild-type CGTase. The dashed line indicates the best fit line through Y195 mutants and wt. The solid line is the best fit line through all the data.)

How Good a Transition State Analogue Inhibitor Is Acarbose? Some measure of the degree to which acarbose mimics the reaction transition state is provided by the plot of log (K_m/k_{cat}) for αG3F versus log K_i for acarbose in Figure 5A. A respectable correlation ($r = 0.90$) is observed with a slope of 1.61 (solid line, all data points), clearly indicating a substantial degree of mimicry. Changes in binding interactions to the inhibitor therefore correlate quite well with changes in transition state binding interactions with substrate. Not surprisingly, there is also some mimicry of ground-state binding interactions as revealed by the correlation of log K_m for the substrate αG3F with log K_i for acarbose (Figure 6A).

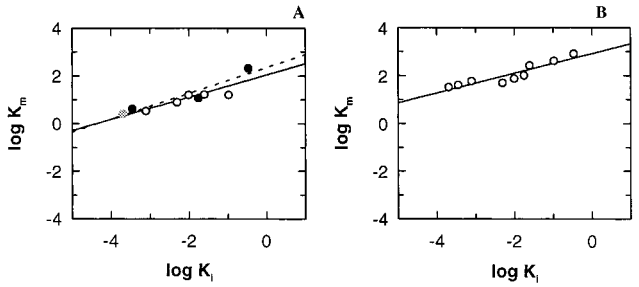

FIGURE 6: Linear free energy relationship between kinetic parameters for the inhibitor acarbose and glycosyl fluoride substrates with a series of mutants of CGTase. (A) log K_m for αG3F vs log K_i for acarbose; (B) log K_m for αGF vs log K_i for acarbose. (Filled circles represent Tyr mutants. The grey shaded circle represents wild-type CGTase. The dashed line indicates the best fit line through Y195 mutants and wt. The solid line is the best fit line through all the data.)

A correlation coefficient of $r = 0.90$ is again observed, but the slope, 0.47, is approximately 3 times smaller than that with log (K_m/k_{cat}).

Interestingly, the correlation seen between K_i for acarbose and K_m/k_{cat} for αGF is considerably better, with $r = 0.98$ and a slope of 2.2, as shown in Figure 5B. This very strong correlation clearly indicates that acarbose has properties of a transition state analogue. Again, some ground-state mimicry was observed, the plot of log K_m versus log K_i for acarbose having a slope of 0.4 and $r = 0.93$ (Figure 6B). A better indication of the relative qualities of these two fits is obtained from the coefficient of determination, r^2. For the K_m/k_{cat} plot, the r^2 value is 0.96, meaning that 96% of the points are well described by the line, whereas for the K_m plot the r^2 value is 0.86, meaning that only 86% of the points are well fit. The better correlation observed for αGF than αG3F is completely consistent with the binding modes of these substrates and of acarbose, as shown in Figure 1. The only occupied subsite common to the substrates and to acarbose is, in fact, the −1 subsite, assuming that acarbose binds in that mode. Thus, the effects of mutations upon interactions at that site will dominate the correlation. Such effects will be particularly large if the mutation directly removes interactions at that site. In addition, changes in interactions at that site resulting from more remote mutations will also be sensed. However, mutations at more remote sites which do not have an effect upon interactions at that site will not be sensed. Thus, mutations affecting only interactions at the +1, +2, and +3 sites will affect the binding of acarbose but will not necessarily affect K_m/k_{cat}

values for the two substrates. This will result in scatter in the plots shown (Figure 5A). Similarly, mutations affecting interactions in the −2 and −3 sites will affect K_m/k_{cat} values for αG3F, but not K_i values for acarbose, thus adding additional scatter to that correlation. The −2 and −3 sites are not directly probed by αGF, hence the improved correlation.

Another measure of the importance of probing equivalent interactions with the substrate and with the inhibitor is obtained by selecting data only for mutants in which interactions at the common (−1) subsite are directly affected. The only amino acid residue mutated which fully fits that requirement is Tyr195. Indeed, as shown with the filled circles in Figure 5A, when only such data are considered a much better correlation ($r = 0.97$, slope = 1.55, linear fit displayed as a dashed line) is observed, consistent with the interactions observed crystallographically.

It is instructive to consider the true meaning of the slopes of these linear free energy relationships, which compare inhibitor binding free energies with activation free energies for the reaction, mutant by mutant. A slope of 1.0 would indicate optimal transition state mimicry since this would indicate that mutations cause equal changes in the binding of the transition state analogue and the transition state itself. Any slope greater or smaller than this would indicate a lesser degree of mimicry. It is not, however, clear that a slope of 1.0 is *required* to indicate any degree of mimicry as has been suggested (*9*), a conclusion that was developed on the assumption of direct proportionality of rate constants and equilibrium constants themselves. The slopes observed for the K_m/k_{cat} plots (1.6−2.2) are therefore approximately equally dissimilar to those observed for the K_m plots (a factor of 2 in each case), perhaps indicating equal mimicry of the ground state and transition state. However it is also quite possible that the large slope in the K_m/k_{cat} plot reflects the fact that acarbose has three sugar residues bound in the +1, +2, and +3 sites which are not occupied in the substrate case. This may well have the effect of immobilizing the valienamine moiety at the active site to a greater extent than is the case for the monosaccharide transition state. A consequence of this could be a greater effect of specific mutations on the binding of this valienamine moiety than on the stabilization of the transition state for glucosyl transfer, hence a slope greater than 1.

Crystallographic Re-refinement. In light of the results presented here which confirm that acarbose has significant transition state analogue character, the binding mode of acarbose to CGTase was reexamined using the original data set as described under Materials and Methods. This is particularly important since, at the time of publication of the first structure (*16*), it was not realized that acarbose may undergo a transglycosylation reaction in the crystal, adding a glucose residue to the valienamine (*26*). The refined structure presented contains all 686 amino acids, 2 Ca^{2+} ions, 1 rearranged acarbose inhibitor, and maltose residues at binding sites (MBS) 1 and 3. At MBS2, originally a maltose was modeled in this position (*16*), but upon refinement, electron density corresponding to four glucose residues was noted. The coordinates of this structure (2cxg) will be submitted to the PDB. The coordinates of an acarbose-derived maltononaose inhibitor bound to CGTase (1dij) (*26*) will also be resubmitted (2dij), since in this instance the valienamine is also modeled at subsite −2 and the 6-deoxyglucose at subsite −1.

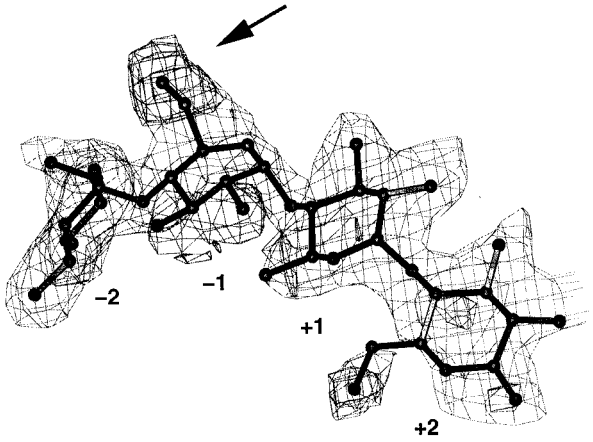

FIGURE 7: Electron density for a rearranged acarbose from the re-refined data set. An arrow indicates the 6-hydroxyl group of the valienamine moiety.

To reexamine the binding mode of acarbose, the electron density maps were calculated using structures refined with the carbohydrate O6 atoms set to zero occupancy. The OMIT (*43*) and SIGMAA (*44*) procedures were used to minimize model bias. The overall statistics (Table 1) show that the old and new structures have a comparable fit to the crystallographic data. However, the electron density calculated after minimizing the refinement bias clearly showed sugar 6-hydroxyl groups at subsites −2, −1, and +2, contradicting the presence of a 6-deoxyglucoside at the −1 site, as originally modeled (Figure 7) (*16*). At subsite +1, electron density for a 6-hydroxyl group is absent. This conclusion was further supported by a 2.2 Å resolution data set from a CGTase I145 mutant complexed to acarbose in which the valienamine moiety was also observed to bind at the −1 subsite (R. Ruiterkamp, unpublished results). Therefore, the 6-deoxyglucose unit of acarbose was modeled into the +1 subsite, and the valienamine unit (which has a 6-hydroxyl group) was modeled into subsite −1, corresponding to the orientation found in α-amylases and other CGTases.

On the basis of this re-refined structure, it is of interest to consider the interactions between the protein and the valienamine moiety in the −1 site that might be responsible for this strong correlation, hence for stabilization of the normal transition state. Probably of primary importance are the hydrogen bonding interactions (3.3 and 2.9 Å, respectively) between OE1 and OE2 of Glu257, the acid/base catalyst, and the NH group of the valienamine. Also of importance, especially given the ring flattening that must occur during catalysis, are the interactions between Asp328 (OD2) and O2 of the valienamine (2.7 Å) as well as between Asp328 (OD1) and O3 of the valienamine (3.2 Å). Other interactions are between His327 (NE2) and both O2 and O3 of the valienamine (3.1 and 3.0 Å, respectively), and between His140 and O6. Interesting stacking interactions also appear to exist between the double bond of the valienamine moiety and the aromatic ring of Tyr100. This substantial network of interactions presumably provides the stabilization needed at the transition state and for binding of this analogue.

Conclusions. The excellent correlation seen between log (K_m/k_{cat}) for hydrolysis of αGF by a series of CGTase

mutants and log K_i for acarbose for each of these same mutants provides good evidence that acarbose functions, at least in part, as a transition state analogue inhibitor for this enzyme. It seems probable that the majority of the binding interactions providing this high affinity are associated with the valienamine moiety. Since acarbose also contains a trisaccharide portion, it is not surprising that it also exhibits ground-state mimicry as revealed in the plot of log K_m versus log K_i. These results are consistent with expectations regarding the structure of the transition state for this retaining transferase. It is also of importance to note that a similar correlation was recently observed for the inverting α-glycosidase, glucoamylase (*15*). These results therefore provide further support for the notion that transition states for inverting and retaining glycosidases are quite similar in character (*45*, *46*). This study also provides a clear example of how detailed kinetic analysis can provide a critical assessment of published crystallographic data resulting in reevaluation of the structural results.

ACKNOWLEDGMENT

We gratefully thank Dr. Dirk Penninga and Prof. Lubbert Dijkhuizen, University of Groningen, The Netherlands, for generous donation of CGTases and Miles Inc. for generous provision of acarbose. We also thank Dr. Paul Bartlett for helpful discussions.

REFERENCES

1. Davies, G. J. (1997) *Biochem. J 321*, 557−559.
2. Pauling, L. (1946) *Chem. Eng. News 24*, 1375−1377.
3. Lienhard, G. E. (1973) *Science 180*, 149−154.
4. Wolfenden, R. (1976) *Annu. Rev. Biophys. Bioeng. 5*, 271−306.
5. Legler, G. (1990) *Adv. Carbohydr. Chem. Biochem. 48*, 319−385.
6. Ganem, B., & Papandreou, G. (1991) *J. Am. Chem. Soc. 113*, 8984−8985.
7. Ermert, P., Vasella, A., Weber, M., Rupitz, K., & Withers, S. G. (1993) *Carbohydr. Res. 250*, 113−128.
8. Wong, C.-H., Provencher, L., Porco, J. A., Jung, S.-H., Wand, Y.-F., Chen, L., Wang, R., & Steensma, D. H. (1995) *J. Org. Chem. 60*, 1492−1501.
9. Mader, M. M., & Bartlett, P. A. (1997) *Chem. Rev. 97*, 1281−1301.
10. Bartlett, P. A., & Marlowe, C. K. (1983) *Biochemistry 22*, 4618−4624.
11. Mookthiar, K. A., Grobelny, D., Galardy, R. D., & Van Wart, H. E. (1988) *Biochemistry 27*, 4299−4304.
12. Hanson, J. E., Kaplan, A. P., & Bartlett, P. A. (1989) *Biochemistry 28*, 6294−6305.
13. Namchuk, M. (1993) Ph.D. Thesis, University of British Columbia.
14. Phillips, M. A., Kaplan, A. P., Rutter, W. J., & Bartlett, P. A. (1992) *Biochemistry 31*, 959−963.
15. Berland, C. R., Sigurskjold, B. W., Stoffer, B., Frandsen, T. P., & Svensson, B. (1995) *Biochemistry 34*, 10153−10164.
16. Strokopytov, B., Penninga, D., Rozeboom, H. J., Kalk, K. H., Dijkhuizen, L., & Dijkstra, B. W. (1995) *Biochemistry 34*, 2234−2240.
17. Schmid, G. (1989) *Trends Biotechnol. 7*, 224−248.
18. Bender, H. (1990) *Appl. Microbiol. Biotechnol. 34*, 229−230.
19. Penninga, D., Strokopytov, B., Rozeboom, H. J., Lawson, C. L., Dijkstra, B. W., Bergsma, J., & Dijkhuizen, L. (1995) *Biochemistry 34*, 3368−3376.
20. Penninga, D., van der Veen, B. A., Knegtel, R. M., van Hijum, S. A., Rozeboom, H. J., Kalk, K., Dijkstra, B., & Dijkhuizen, L. (1996) *J. Biol. Chem. 271*, 32777−32784.
21. Wilcox, E. R., & Whitaker, R. J. (1984) *Biochemistry 23*, 1783−1791.
22. Svensson, B., & Sierks, M. R. (1992) *Carbohydr. Res. 227*, 29−44.
23. Baliga, B. S., & Fonseca, V. A. (1997) *Am. Fam. Physician 55*, 817−824.
24. Scheen, A. J. (1997) *Drugs 54*, 355−368.
25. Yee, H. S., & Fong, N. T. (1996) *Pharmacotherapy 16*, 792−805.
26. Strokopytov, B., Knegtel, R. M. A., Penninga, D., Rozeboom, H. J., Kalk, K. H., Dijkhuizen, L., & Dijkstra, B. W. (1996) *Biochemistry 35*, 4241−4249.
27. Aleshin, A. E., Firsov, L. M., & Honzatko, R. B. (1994) *J. Biol. Chem. 269*, 15631−15639.
28. Qian, M., Haser, R., Buisson, G., Duee, E., & Payan, F. (1994) *Biochemistry 33*, 6284−6294.
29. Brzozowski, A. M., & Davies, G. J. (1997) *Biochemistry 36*, 10837−10845.
30. Wind, R. D., Uitdehaag, J. C., Buitelaar, R., Dijkstra, B. W., & Dijkhuizen, L. (1998) *J. Biol. Chem. 273*, 5771−5779.
31. Mosi, R., He, S., Uitdehaag, J., Dijkstra, B., & Withers, S. G. (1997) *Biochemistry 36*, 9927−9934.
32. Knegtel, R. M., Strokopytov, B., Penninga, D., Faber, O. G., Rozeboom, H. J., Kalk, K. H., Dijkhuizen, L., & Dijkstra, B. W. (1995) *J. Biol. Chem. 270*, 29256−29264.
33. Junnemann, J., Thiem, J., & Pedersen, C. (1993) *Carbohydr. Res. 249*, 91−94.
34. Leatherbarrow, R. J. (1994) Gra-Fit, Version 3.0, Erithacus Software Ltd., London, U.K.
35. Brünger, A. T. (1997) *Methods Enzymol. 277*.
36. Tronud, D. E., Ten Eyck, L., & Matthews, B. W. (1987) *Acta Crystallogr. A43*, 489−501.
37. Jones, T. A., Zou, J. Y., Cowan, S. W., & Kjedgaard, M. (1991) *Acta Crystallogr. A47*, 110−119.
38. Laskowski, R. A., MacArthur, M. W., Moss, D. S., & Thornton, J. M. (1993) *J. Appl. Crystallogr. 26*, 283−291.
39. Hooft, R. W. W., Vriend, G., Sander, C., & Abola, E. E. (1996) *Nature 381*, 272.
40. Kempton, J. B., & Withers, S. G. (1992) *Biochemistry 31*, 9961−9969.
41. Namchuk, M. N., & Withers, S. G. (1995) *Biochemistry 34*, 16194−16202.
42. Tull, D., & Withers, S. G. (1994) *Biochemistry 33*, 6363−6370.
43. Vellieux, F. M. D., & Dijkstra, B. W. (1997) *J. Appl. Crystallogr. 30*, 396−399.
44. Read, R. J. (1986) *Acta Crystallogr. A42*, 140−149.
45. Tanaka, Y., Tao, W., Blanchard, J. S., & Hehre, E. J. (1994) *J. Biol. Chem. 269*, 32306−32312.
46. Wang, Q., Graham, R. W., Trimbur, D., Warren, R. A. J., & Withers, S. G. (1994) *J. Am. Chem. Soc. 116*, 11594−11595.
47. Luzzati, V. (1952) *Acta Crystallogr. 5*, 802−810.

BI981109A